



ELSEVIER

Contents lists available at ScienceDirect

Case Studies in Construction Materials

journal homepage: www.elsevier.com/locate/cscm

Case study

Strengthening of damaged low strength concrete beams using PTMS or NSM techniques

Thanongsak Imjai^{a,*}, Monthian Setkit^a, Reyes Garcia^b, Fabio P. Figueiredo^c^a School of Engineering and Technology, and Center of Excellence in Sustainable Disaster Management, Walailak University, Nakhon Si Thammarat, 80160, Thailand^b School of Engineering, The University of Warwick, Coventry, CV4 7AL, UK^c School of Engineering, University of Minho, Guimarães, 4800-058, Portugal

ARTICLE INFO

Article history:

Received 27 February 2020

Received in revised form 25 June 2020

Accepted 25 June 2020

Keywords:

Flexural strengthening
Low strength concrete
Post-Tensioned Metal Strap
Side Near Surface Mounted
FRP

ABSTRACT

This article presents the results of an analytical and experimental study on the performance of rectangular reinforced concrete (RC) beams strengthened using either post-tension metal strapping (PTMS) or side-near surface mounted (SNSM) FRP bars. Four low-strength (15.3 MPa) medium-scale beams were tested in four-point bending in two phases. In Phase I, one control beam was tested up to failure, whereas three beams were tested up to yielding of the main flexural reinforcement. In Phase II, the three pre-cracked beams were strengthened using PTMS or SNSM techniques, and then retested up to failure. The results indicate that the capacity of the pre-cracked PTMS-strengthened beam was only 8 % higher than the control counterpart. Conversely, the SNSM strengthening solution increased the beam capacity by up to 55 %, which is due to additional flexural reinforcement provided by the FRP bars. Moreover, the predictions given by linear cracked sectional analysis and the current ACI guidelines match well the deflection response of the strengthened beams but only up to the yielding load.

© 2020 The Author(s). Published by Elsevier Ltd. This is an open access article under the CC BY-NC-ND license (<http://creativecommons.org/licenses/by-nc-nd/4.0/>).

1. Introduction

In many circumstances, reinforced concrete (RC) elements may crack even at service load conditions, which can lead to corrosion in the reinforcement once moisture reaches the steel bar. Several solutions (such as epoxy injection or bar epoxy coating) have been proposed to overcome this problem. However, once cracks develop, the capacity of such elements reduces. Previous research has shown that the use of advanced composite materials was effective at strengthening pre-cracked concrete elements, and have also successfully restored their designed section capacity and meet serviceability requirements [1–5].

Previous research [6] led to the development of the original Post-Tensioned Metal Strapping (PTMS) technique, whereas recent extensive experimental work at Walailak University [7] led to the development of a highly durable ductile PTMS technique. The technique uses ductile high-strength steel straps post-tensioned around RC elements using strapping tools as those used in the packaging industry. Pneumatic tools are used to apply the tension force into the metal straps, and thus the applied force is regulated accurately. This method has proven effective in strengthening medium-scale RC members

* Corresponding author.

E-mail address: thanongsak.im@wu.ac.th (T. Imjai).

subjected to monotonic and seismic loading [8–11]. The low cost of the materials and the ease and speed of application make this technique very effective for the repair and strengthening of existing deficient RC structures.

Near-surface mounted (NSM) systems involve the insertion of Fibre Reinforced Polymer (FRP) strips or bars into pre-cut grooves filled with epoxy adhesive [12–14]. Past research has proven the effectiveness of NSM FRP in RC beams strengthened in flexure [12,15–17]. The results from these studies indicate that the flexural capacity of NSM FRP-strengthened specimens increases between 30–70 % over control specimens, thus making NSM a very attractive strengthening solution. NSM systems are usually applied at the soffit of RC beams or slabs. This implies that such elements should be wide enough to accommodate the necessary edge clearance and clear spacing between adjacent NSM grooves [1,13]. However, in many structures, beams and slabs hold suspended ceilings, air ducts, extractors and electrical wiring at their soffit [17], which reduces the area in which the NSM FRP system can be mounted. Consequently, it is necessary to explore alternative strengthening locations (other than the soffit) so as to make NSM FRP systems more versatile.

This article investigates the performance of precracked concrete beams strengthened with post-tension metal strapping and side-near surface mounted FRP techniques. In Phase I, beam B0 (control specimen) was tested up to failure, whereas beams B1 to B3 were pre-loaded up to yielding. In Phase II, the pre-cracked beams (tested in Phase I) were strengthened using a PTMS technique or using side-near surface mounted CFRP bars. The experimental results are discussed in terms of observed damage, load-deflection behaviour, stiffness loss and energy dissipation capacity. The effectiveness of sectional analysis (according to the current design guidelines) at predicting the load-deflection response of the beams is also briefly discussed.

2. Experimental programme

The experimental work involved the preparation and testing of four concrete beams reinforced with flexural and shear steel reinforcement. All beams were under-reinforced in flexure. The beams were tested in four-point bending in two testing Phases:

- Phase I: Beam was B0 tested up to failure. Beam specimens B1, B2 and B3 were tested up to the load level that induced yielding in the flexural reinforcement according to the ACI 318 design provision [18].
- Phase II: specimens B1 to B3 were strengthened using different solutions, and subsequently re-tested.

2.1. Test matrix and reinforcement details

All beam specimens had a rectangular cross-section of 150×250 mm with a clear span of 2300 mm. Control beam B0 was first tested up to failure, whereas beams B1, B2 and B3 were subjected to the two consecutive phases of testing: The tested beams had internal flexural and shear steel reinforcement, designed according to the specifications of the current ACI Building code (ACI 318-19). To promote a flexural dominated behaviour, each beam was subjected to four-point bending with a shear span to effective depth ratio (a/d) equal to 3.65. Accordingly, the beams can be classified as Type II in Kani's shear valley and therefore the "beam action" will be a combination of shear and flexure. In reality, beams are always subjected to both flexural and shear load and thus the a/d ratio selected in this study favours the failure in a combined flexural and shear mode. However, all specimens were designed to fail in flexure by providing sufficient shear reinforcement (stirrups) according to current design guidelines

Two $\emptyset 12$ mm steel reinforcement ($f_y=392$ MPa) were used as flexural bottom reinforcement in all of beam specimens, thus leading to a flexural reinforcement ratio $\rho_f=0.73$ %. The provided flexural reinforcement ratio was greater than the ACI minimum and approximately equal to 68.9 % of the ACI maximum longitudinal reinforcement ratio. The top reinforcement in the compression zone (on the shear span) consisted of two $\emptyset 9$ mm bars ($f_y = 235$ MPa), which also held the vertical shear stirrups. Shear failure was prevented by adding two-legged steel stirrups of $\emptyset 9$ mm at a spacing of 100 mm ($\rho_w = 0.84$ %) between centres. Table 1 presents a summary of the details of the beams used in this experimental programme. The acronym

Table 1
Characteristics of tested beam specimens.

Phase	Beam ID	Condition	Remarks
I	B0	As built	Control beam and tested up to failure
	B1	As built	Tested up to 100 % P_y
	B2		
	B3		
II	B1-PTMS	Precracked + PTMS confinement	Damaged beam B1 strengthened with PTMS
	B2-SNSM	Precracked + SNSM at top side	Damaged beam B2 strengthened with SNSM at compression side
	B3-SNSM	Precracked + SNSM at bottom side	Damaged beam B3 strengthened with SNSM at tension side (soffit)

Note: PTMS = Post-Tensioned Metal Strapping; SNSM = Side Near-Surfaced Mounted FRP; P_y = load level where the longitudinal reinforcement reaches approximately 2000 microstrains (yielding load).

in the beam ID refers to the two strengthening techniques examined in the study, either Post-Tensioned Metal Strapping (PTMS) or Side Near Surface Mounted (SNSM) strengthening. The strengthening solutions are discussed later in the article.

2.2. Concrete properties

Ordinary Portland Cement (OPC type I) was used to cast the beam, cylinder and prism specimens. The mix design for the concrete is shown in Table 2. Crushed granite stone with a maximum size of 10 mm was used as coarse aggregate, and river sand was used as fine aggregate. The water-to-cement ratio (w/c) was 0.77 with a slump of 75 mm. The target strength of concrete used in this study was 15 MPa and the properties of concrete were determined according to the British Standards [19–21]. The average compressive strengths of concrete obtained from 150×300 mm cylinders and 150 mm cubes measured at the time of testing were 15.3 MPa and 17.1 MPa, respectively. The indirect tensile splitting strength ($f_t = 1.6$ MPa) was determined from tests on six 150×300 mm cylinders. The flexural strength ($f_b = 1.9$ MPa) was obtained from four-point bending tests on three prisms of $100 \times 100 \times 500$ mm. All cubes, cylinders and prisms were cast at the same time and cured together with the beams. Table 3 summarises the properties of the concrete used in this study.

2.3. Test setup and instrumentation

The beams were tested in four-point bending to produce a constant moment region at the midspan. The beams were simply supported on steel plates and rollers. The tests were performed using a Universal testing Machine (UTM) with a maximum capacity of 1,000 kN in a displacement control mode at a rate of 1 mm/min. Overall beam deflections were measured using Linear Variable Displacement Transducers (LVDTs), as shown in Fig. 1. Strain gauges were located on the flexural reinforcement within the midspan to monitor the strain of the longitudinal reinforcement where the maximum strain caused by pure flexure was expected. Additional LVDTs were positioned at midspan, under the point loads. Two additional LVDTs were placed on the top face of each of the beam supports to allow for the calculation of net deflections.

In testing Phase I, for specimens B1 to B3, the load was applied automatically in displacement control mode in increments of approximately 1 mm/min. At each loading step, the load was halted, cracks were marked and the width of selected cracks was measured using a hand held micrometer every 5 or 10 kN, depending on the expected load capacity of the beam. For the control specimen B0, the load was then applied until failure of the beam. Beams B1 to B3 were loaded up to a load (P_y) that produced yielding of the flexural reinforcement (strain gauge readings of approximately 0.002). The selected preload level P_y in Phase I exceeded the service load and aimed to produce significant but still repairable damage in the beams, which in turn avoided the need of performing crack injections or epoxy mortar patching. Accordingly, such preload level is representative of a condition at which strengthening of the beams is absolutely necessary to ensure their structural integrity. In testing Phase II, each of the pre-cracked beam specimens (B1-PTMS, B2-SNSM, and B3-SNSM) was tested up to failure, and all cracks were marked and recorded (similar to Phase I).

3. Strengthening of precracked concrete beams

Before retesting beams B1 to B3 in Phase II, such pre-cracked beams were strengthened using different solutions. B1 was strengthened using Post-Tensioned Metal Straps at the constant moment region and renamed as B1-PTMS in Phase II. Beams B2 and B3 were strengthened using side-near surface mounted Carbon FRP (CFRP) bars at the compression and tension side of the section, respectively and renamed as B2-SNSM and B3-SNSM (see Section Y-Y in Fig. 1). The adopted strengthening solutions are described in the following sections.

Table 2
Concrete mix proportion.

Mix proportion (kg/m ³)				w/c ratio	Slump (mm)
Cement	Coarse aggregate	Fine aggregate	Water + Plasticiser		
250	120	757	200	0.77	75

Table 3
Mechanical properties of concrete.

Statistical values	Cylinder compressive strength (f_c)	Cube compressive strength ($f_{c,cube}$)	Tensile strength (f_t)	Modulus of rupture (f_b)
Mean (MPa)	15.3	17.1	1.4	1.9
Std. Dev. (MPa)	2.3	3.5	0.5	0.2
Samples (No.)	6	6	6	6

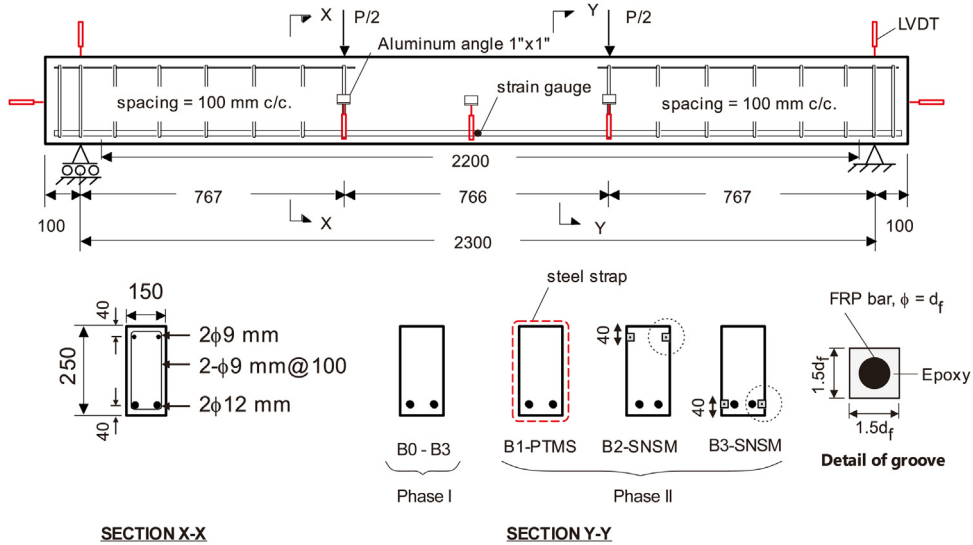


Fig. 1. Reinforcement details of tested beams and instrumentation (units: mm).

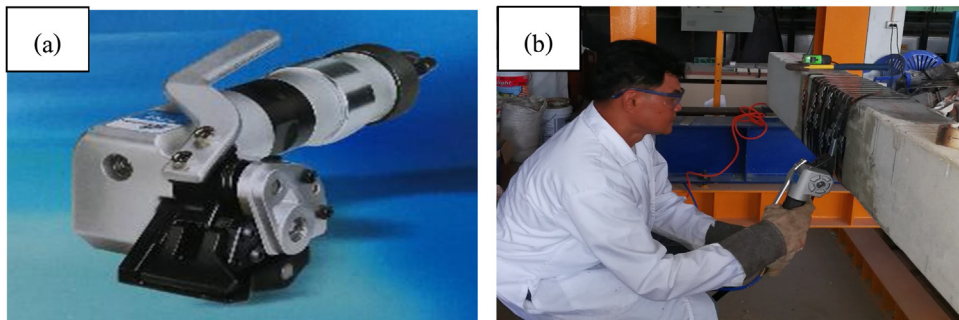


Fig. 2. Strapping pneumatic model PT-52 (a) and strengthening of cracked beam B1-PTMS at midspan using a pneumatic air pressure tool (b).

3.1. Strengthening of beam B1 using PTMS technique

The main purpose of adding PTMS confinement was to increase the deformation capacity of the concrete above the neutral axis (which is subjected to compression), and thus increase the beam's ductility.

The straps had a cross section of 25×0.9 mm and were fixed using a pneumatic strapping tool model PT-52 at a pressure of 8 bars (116 psi), as shown in Fig. 2a, b. The highly ductile metal straps had an epoxy coated and wax finishing. The elongation at break of the metal straps was 9.6 %, whereas their average yield stress and ultimate stress obtained from six direct tensile tests were 850 MPa and 950 MPa, respectively. The number and spacing of the straps was chosen to produce a modest value of confinement ratio ω_c ($\omega_c = A_s f_{ys} / A_c f_c$, where A_s and A_c are the areas of straps and confined concrete respectively, and f_{ys} is the yield strength of the straps). The centre to centre spacing s between straps was 35 mm, thus leading to a value $\omega_c = 0.14$. In actual confinement applications, designers can choose the confinement ratio ω_c by changing the strap spacing, number of strap layers, and yield strength of the straps.

To maintain the tensioning force after post-tensioning, the straps were fastened mechanically using jaws and metal clips. This provides active confinement to the beam. The clip efficiency is also affected by the type and operational condition of the sealing machine used. The efficiency with single or double notch sealing depends on the friction induced as a result of the out of plane bending of the clip. This out of plane bending is associated with rupture of the strip and, therefore, the reduction of its dimensions and ultimate strength. Extensive research by Imjai et al. [7] improved the effectiveness of the PTMS system by avoiding the rupture of the strip at two positions, which occurs in single notch connections. Accordingly, double notch connections were applied during the fastening process of PTMS system (see Fig. 3b). The reduced prestressing force in the strip was measured following the sealing application. This is due to the lifting imposed on the strip during the sealing of the clip by the sealing tool. Stress relaxation tests due to creep effects were also performed to investigate the reduction of prestress force in six coupons (25×0.9 mm strip) secured with single or double notch metal clips. The setup shown in Fig. 3a was used to perform creep tests for 30 days at an initial stress of 330 MPa, and the results are compared in Fig. 3b. The

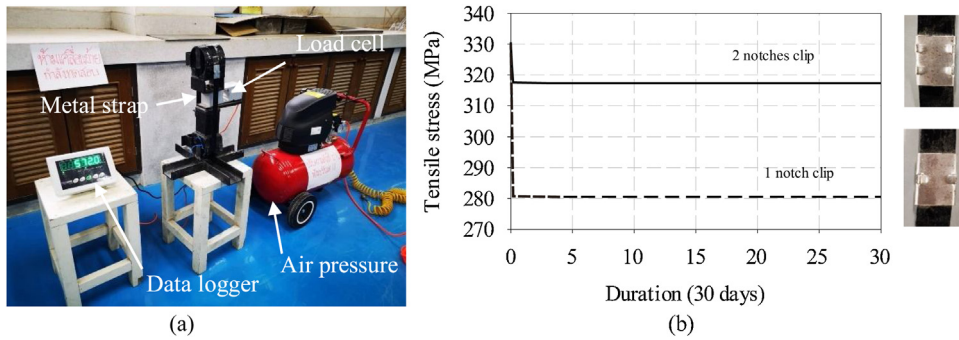


Fig. 3. Creep tests (a) and stress relaxation test results over a 30 days period (b) (adapted from Imjai et al. [7]).

results indicate that the average prestress loss after sealing the clips was approximately 4% and 15% for the double and single notch sealing, respectively. Accordingly, a double notch sealing was used in this study to guarantee that the pre-tension stress remained at approximately 315 MPa during the test of B1-PTMS (Phase II). Note that all metal straps were removed for crack inspection after the test in Phase II.

It should be also mentioned that, in real strengthening applications, the top of the RC beam may not be accessible for complete wrapping of the metal straps. In this case, two solutions are possible:

- 1 To use mechanical anchors (e.g. bolts and steel plates) to support the straps and hold the tensioning force, which proved extremely effective in a strengthening application on beams and beam-column joints [22], or
- 2 To open slots by drilling through the top of the slab, making sure that the slab reinforcement does not damage during the operation.

3.2. Strengthening of beams B2 and B3 using side-near surface mounted (SNSM) technique

The SNSM technique was used to strengthen the pre-cracked beams B2 and B3 tested in Phase I. In the strengthening procedure, two CFRP bars were installed into grooves in a longitudinal direction on both sides at 40 mm below the top face of beam B2, and at 40 mm above the soffit of beam B3 (see Fig. 1). The grooves were cut in the concrete cover using a diamond blade and the groove dimensions specified in ACI 440.2R [1]. The grooves were cleaned with a high-pressure air jet and acetone. Finally, the grooves were half-filled with epoxy adhesives and the CFRP bars were pushed into the grooves with slight force as shown in Fig. 4. It should be noted that the strengthening solution adopted for beam B2 (renamed B2-SNSM in Phase II) is somehow unusual due to the fact that the FRP bars were located on the compression zone of the beam. The purpose of this adopted solution was to replicate the strengthening of an inverted RC beam with limited lateral access due to the potential presence of a slab. This type of beams are found in existing buildings of many developing countries, including Thailand. Whilst not ideal, in this case it would only be possible to apply NSM FRP on the compression zone of the beam. However, this solution is expected to have a marginal effect on the capacity enhancement of beam B2-SNSM. It should be also mentioned that whilst the strengthening solution used for B1-PTMS aimed at enhancing ductility, the goal of the NSM FRP interventions on beams B2-SNSM and B3-SNSM was to increase the beams' capacity. As such, the strengthening solutions are not directly comparable.

Sand coated CFRP bars (fibre volume = 68 %) with a diameter (d_f) of 8 mm was used for the SNSM strengthening solutions by inserting into pre-cut grooves of $1.5d_f$ (see Fig. 1). The 8 mm bar size was chosen due to practical reasons: a) a larger bar size would have required a deeper side groove, thus risking damaging/cutting the existing steel stirrups, and b) the tools available in the laboratory were just enough to cut the side groove with a width of $1.5d_f$. This led to a modest reinforcement ratio

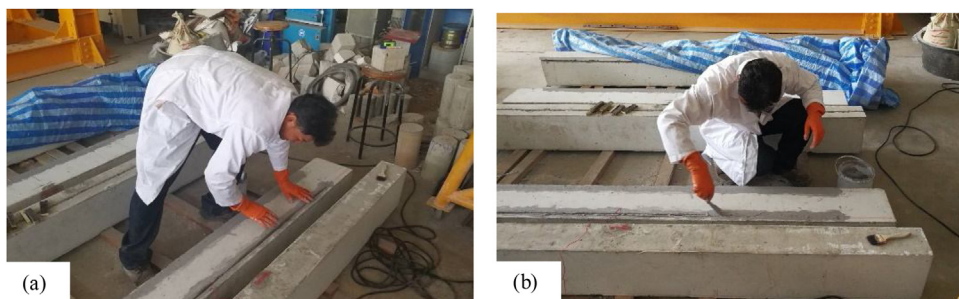




Fig. 4. Placing CFRP into the pre-cut grooves (a) and fully filled the grooves with epoxy adhesive (b).

Table 4
Sand-coated CFRP bar and epoxy adhesive for SNSM strengthening work.

Sand coated CFRP bar	Epoxy adhesive Parts A & B	Mechanical properties	
		Compressive strength	95 MPa
		Tensile strength	31 MPa
		Shear strength	19 MPa
		Elastic modulus	11,200 MPa

of CFRP $\rho_f = 0.0029$. The mechanical properties of the CFRP bars were determined from tensile tests on six coupons, having 2,206 MPa of nominal tensile strength, and 174.6 GPa of modulus of elasticity with an elongation at break of 1.5 %. Two-part commercially available epoxy adhesive was used to bond the composite reinforcement to the concrete. The epoxy adhesive consisted of two parts (A-white: B-black) which were mixed in a ratio of 3:1 using a rotary mixing tool until a uniform grey colour was achieved. The adhesive had 19 MPa of shear strength, and 11.2 GPa of modulus of elasticity, according to the manufacturer's specifications. The epoxy bond strength for concrete and steel was 4 and 21 MPa, respectively. Mechanical and physical properties of epoxy adhesive after 7 days, as given by the manufacturer, are shown in Table 4.

4. Test results and discussion

4.1. Capacity and failure modes

Table 5 summarises the experimental results in terms of the cracking load (P_{cr}), yield load (P_y), ultimate load (P_u), ultimate deflection at midspan (δ_{max}), maximum measured crack width (w_f) and failure mode (SY = steel yielding, CC = concrete crushing). In Phase I, the loading was halted when the flexural strain exceeded 0.002. The values w_f shown in Table 5 were measured at the load level that was deemed safe to take a last reading. In Phase II, the ultimate loads of the strengthened specimens are presented together with the maximum midspan deflections.

In Phase I, first flexural cracks were observed for the control specimen B0 at the cracking load $P_{cr} = 16.5$ kN. Initially, small narrow flexural cracks developed within the midspan and shear span region. Flexural cracks widened and were visible to the naked eye as the load further increased. The maximum load of beam B0 was 59.5 kN, and the beam 'failure' was dominated by flexural steel yielding (SY) (see Fig. 5a). Specimens B1 to B3 had a similar behaviour to beam B0, with cracking loads of 17.0, 16.8, 16.9 kN and yielding loads of 56.7, 55.9, 56.2 kN for B1, B2 and B3, respectively, accompanied by flexural steel yielding (refer to Fig. 5b–d). Testing was halted when the yield load was reached, after which the cracked specimens were strengthened and renamed.

In testing Phase II and as the load increased, flexural and shear cracks (which developed in Phase I), propagated and penetrated considerably deeper towards the loading points. The measured ultimate capacities of the beams tested in Phase II were 68.2, 65.1, and 98.2 kN for beams B1-PTMS, B2-SNSM, and B3-SNSM, respectively. Failure was dominated by concrete crushing (CC) at the top fibre in beams B1-PTMS (Fig. 6a), B2-SNSM (Fig. 6b), and B3-SNSM (Fig. 6c).

4.2. Performance of strengthened pre-cracked RC beams

Table 6 compares results of the control specimen B0 tested in Phase I with those from the strengthened specimens B1-PTMS, B2-SNSM and B3-SNSM tested in Phase II. The results are compared in terms of ultimate capacities (P_u) and capacities over beam B0 ($P_u/P_{u,B0}$), ductility at ultimate (μ_u), ductility at failure (μ_f), initial stiffness (K_e) and energy absorption (ξ). For the case of specimen B1-PTMS, the results in the table show a marginal increase of 8% in ultimate capacity compared to B0 as the PTMS confinement was not expected to greatly affect the ultimate load. As seen in Table 6, the ultimate load of specimen B2-SNSM is only 3% higher than that of B0. This confirms that the CFRP reinforcement provided in the compression zone has

Table 5
Summary of main results of beams tested in Phases I and II.

Phase	Beam ID	P_{cr} (kN)	P_y (kN)	P_u (kN)	δ_{max} (mm)	w_f (mm) @ P	Failure mode
I	B0	16.8	57.8	63.2	22.4	2.00@50.0 kN	SY
	B1	17.0	56.7	–	10.4	1.55@36.7 kN	SY
	B2	16.8	55.9	–	11.0	1.25@35.9 kN	SY
	B3	16.9	56.2	–	10.5	1.45@36.2 kN	SY
II	B1-PTMS	–	–	68.2	22.0	2.30@50.0 kN	CC
	B2-SNSM	–	–	65.1	34.2	2.45@50.0 kN	CC
	B3-SNSM	–	–	98.2	33.7	2.35@50.0 kN	CC

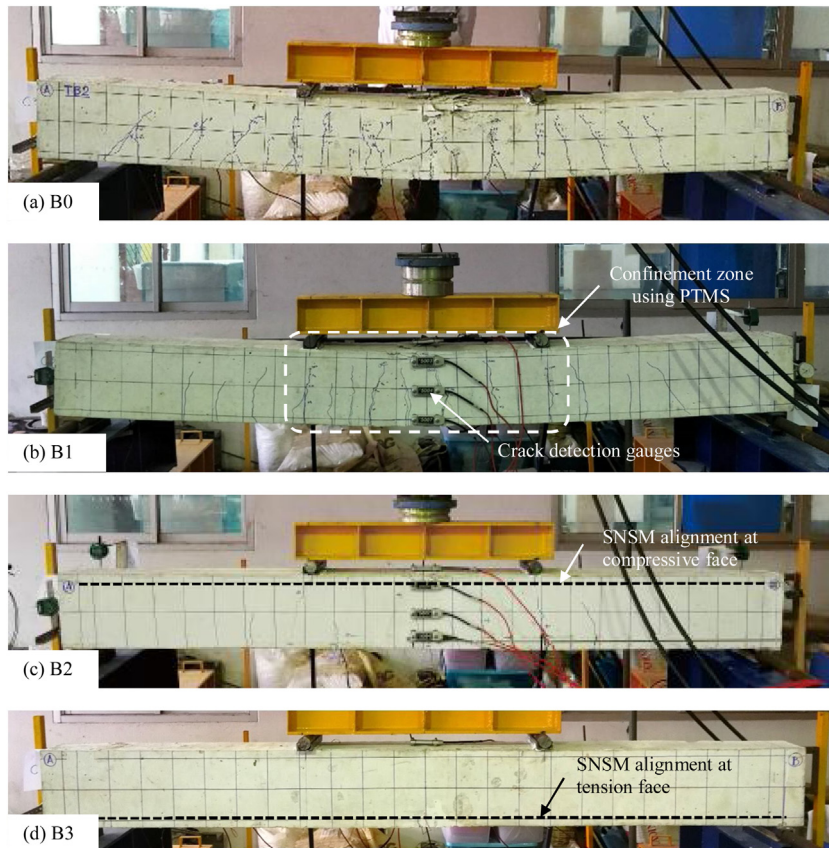


Fig. 5. Failure of control beam B0 (a), and specimens B1 (b), B2 (c), and B3 (d) tested in Phase I.

a negligible effect in flexural strength. The results also show that the ultimate load of B3-SNSM is 55 % higher than that of B0. The increase in flexural capacity in the latter beam is attributed to the additional CFRP reinforcement provided in the strengthening solution.

The ductility at ultimate, μ_u , was determined as the ratio of the deflection at ultimate to the deflection at yield load. The ductility at failure, μ_f , was determined as the ratio of the deflection at failure to the deflection at yield load. Therefore, the ductility index derived from load-deflection curves of the specimens tested in Phase II is the capacity to endure inelastic deformation without reduction of load carrying capacity before failure. The results in Table 6 show that the two beams strengthened with SNSM exhibited greater μ_u and μ_f values compared to B0. This is due to the additional flexural reinforcement in compression or in tension zones provided by SNSM CFRP bars. B2-SNSM exhibits the highest ductility of all the strengthened sections. Surprisingly, the PTMS strengthening only improved the ductility at peak load μ_u of B1-PTMS by 12 %, whereas μ_f reduced by 7 % compared to B0. This can be due to the fact that beam B2 yielded during the tests in Phase I. Regardless of the strengthening solution, all cracked sections strengthened with either PTMS or SNSM reported adequate ductility.

The pre-yield stiffness (K_e) was calculated from the slope of the load-deflection curve in the elastic zone. As expected, all of the strengthened beams tested in Phase II showed a lower K_e compared to the (uncracked) control specimen B0 tested in Phase I. This is due to the fact that such strengthened specimens were already cracked from the tests in Phase I, which significantly affected the initial stiffness of the load-deflection curves in Phase II. The results also show that both PTMS and SNSM strengthening techniques did not change significantly the initial stiffness of the beams, as all of them have a K_e between 22–28 % lower than B0. Specimen B3-SNSM exhibits a slightly higher K_e compared to B1-PTMS and B2-SNSM specimens because the FRP on the tension side of the section improved the beam's initial rigidity and stiffness.

The energy absorption capacity of concrete members is a dominant parameter for the assessment of the toughness or failure behaviour [17]. In this study, the energy absorption capacity per unit area (ξ) of the tested beams was calculated as the area under the load-deflection curve (see Fig. 7). The results show that the energy absorbed by B1-PTMS is 10 % higher than that absorbed by B0. The results in Table 6 also indicate that the strengthened beams B2-SNSM and B3-SNSM had a higher energy absorption capacity by 71 % and 147 % over B0, respectively. The significant enhancement of energy absorption capacity in Beam B3-SNSM relies on the larger improvement of load carrying capacity and stiffness after yielding of the reinforcement, as well as on the higher deflection mobilised in the post-cracked stage.

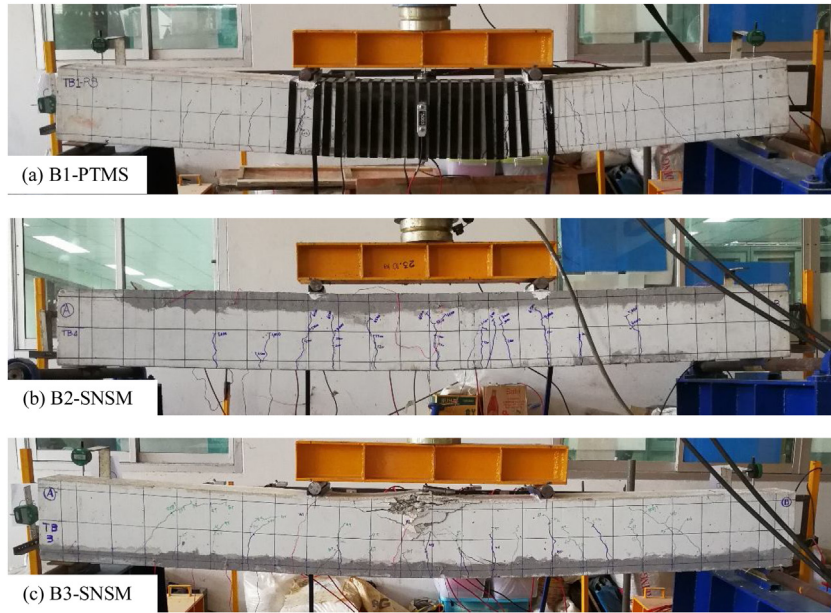


Fig. 6. Failure of strengthened specimens B1-PTMS (a), B2-SNSM (b) and B3-SNSM (c) tested in Phase II.

Table 6

Comparison of ultimate capacity, ductility, stiffness and energy absorption of tested beams.

Phase	Beam ID	P_u (kN)	$P_u/P_{u,B0}$	μ_u	μ_f	K_e (kN/m)	$K_e/K_{e,B0}$	ξ (kN·mm)	ξ/ξ_{B0}
I	B0	63.2	1.00	1.48	1.96	12.9	1.00	4,497	1.00
	B1-PTMS	68.2	1.08	1.66	1.82	9.8	0.74	4,950	1.10
II	B2-SNSM	65.1	1.03	2.72	2.74	9.9	0.76	7,671	1.71
	B3-SNSM	98.2	1.55	2.11	2.53	10.1	0.78	11,130	2.47

Note: μ_u = ductility at ultimate load, μ_f = ductility at failure load, K_e = effective pre-yield stiffness, and ξ = energy absorption.

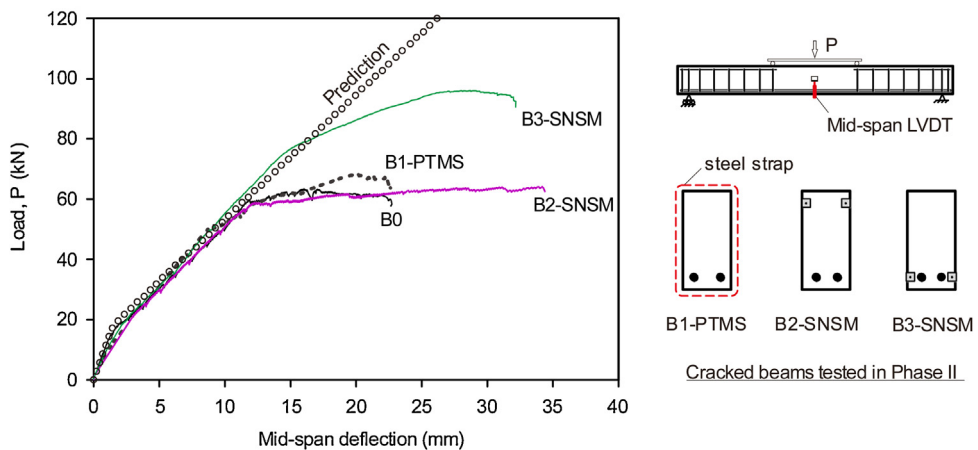


Fig. 7. Experimental deflections of tested beams and ACI 318 code prediction.

4.3. Analysis of beam deflections

Short-term deflections of RC beams are generally derived using linear-elastic deflection equations using an effective moment of inertia to account for loss of stiffness due to cracking. To predict deformation responses of the tested beams, this study focusses on the widely adopted ACI 318 [18] recommendations.

ACI 318 adopts an equation developed originally by Branson [23] for the effective moment of inertia, I_e . The equation provides a transition between the upper and lower bounds of I_g and I_{cr} as a function of the ratio between the cracking moment (M_{cr}) and applied moment (M_a) (Eq. (1)):

$$I_e = \left(\frac{M_{cr}}{M_a}\right)^3 I_g + \left[1 - \left(\frac{M_{cr}}{M_a}\right)^3\right] I_{cr} \quad (1)$$

The total midspan deflection, Δ_{mid} , of rectangular beams subjected to bending and shear forces can be obtained using virtual work principles:

$$\Delta_{mid} = \frac{23PL^3}{1296EI_e} + \frac{k_s PL}{6GA} \quad (2)$$

where P is the total load, L is the clear span of the beam, k_s is the shear correction factor for rectangular sections (6/5 for a rectangular section), A is the cross sectional area of the beam, and E and G are the elastic and shear modulus, respectively ($G = E / 2(1+\nu)$, where ν is the Poisson ratio).

For RC elements, the effective moment of inertia I_e is often used to calculate the flexural deformation component (first term on right hand side of Eq. (2)), whereas the shear component (second term of Eq. (2)) is considered negligible for slender beams (i.e. Model Code 2010 [24]). Fig. 7 compares the load-deflection responses of strengthened specimens (Phase II) and the control specimen B0 (Phase I). For comparison purposes, the figure also shows the (flexural) deflection predictions for B0 calculated according to ACI 318, but ignoring the shear component. It should be noted that the concrete tensile strength used to determine the cracking moment and cracking load was derived from inverse analysis to account indirectly for the variability of concrete, size effects, as well as shrinkage effects on the initial strain state within the element and on the apparent concrete properties. Overall, the results in Fig. 7 indicate that the ACI 318 model predicts reasonably well the deflections up to (low) loads corresponding to service conditions for the control specimen B0 (Phase I).

As seen in Fig. 7, the deflection of strengthened beam specimens can also be adequately predicted by equations included in current guidelines sections between the cracking to yielding load levels. At higher load levels, such equations can significantly underestimate deflections by up to 25 %. Furthermore, the predictions given by the models underestimate considerably deflections at higher loads (i.e. after concrete cracking). Such inconsistencies are due to the formation of shear diagonal cracks at higher load levels, which results in an additional component of deformation. This component is referred to as *shear crack induced deformation*, as reported recently by Imjai et al. [4]. Based on twelve tests from FRP RC beams, the authors reported that the estimated total deflection of strengthened concrete specimens could be significantly improved by adding the component of deflection due to shear action and crack opening to the component due to flexural deflection calculated by existing equations.

5. Conclusions

This article presents the results of an analytical and experimental study on the performance of strengthened pre-damaged low strength concrete beams. The following conclusions can be drawn from the results:

- Significant decrease in initial beam stiffness of strengthened beams compared to the control specimen was reported due to the specimens were already cracked from the tests in Phase I
- The cracked beams strengthened with a modest SNSM strengthening solution exhibited higher capacity (+55 %), ductility and energy absorption compared to the counterpart control beam. This is due to the additional flexural reinforcement provided by the SNSM strengthening solution, and to an enhancement of energy absorption capacity in the post-cracking stage.
- The pre-cracked beam strengthened with SNSM at the tension side of the section shows superior performance over the beam strengthened with SNSM at the compression side.
- Compared to the control specimen, the Post-Tensioned Metal Strapping confinement increased marginally the ductility at peak load (by 12 %), but not the ductility at failure.
- The deflection of strengthened low strength concrete beam specimens can be adequately predicted by equations included in current guidelines sections between the cracking to yielding load levels. At higher load levels, such equations can significantly underestimate deflections by up to 25 %.

Declaration of Competing Interest

The authors have no conflict of interest.

Acknowledgements

The author acknowledges the financial support provided by Walailak University research grant (contract no. WU62227). This research was partially supported by the New Strategic Research (P2P) project, Walailak University, Thailand. The first author thankfully acknowledges the support provided by the TRF mid-career research grant 2020. The authors thankfully acknowledge Mr. Poj Ancharoen's contribution during the experimental programme.

References

- [1] ACI 440.2R-08: Guide for the Design and Construction of Externally Bonded FRP Systems for Strengthening Concrete Structures, 440.2R-08, Farmington Hills, MI, 2008.
- [2] M.A. Morsy, M.E. El-Tony, M. El-Naggar, Flexural repair/strengthening of pre-damaged R.C. beams using embedded CFRP rods, *Alexandria Eng. J.* 54 (4) (2015) 1175–1179.
- [3] A.A. Shukria, M.A. Hosena, R. Muhamad, M.Z. Jumaata, Behaviour of precracked RC beams strengthened using the side-NSM technique, *Constr. Build. Mater.* 123 (1) (2016) 617–626.
- [4] T. Imjai, M. Guadagnini, R. Garcia, K. Pilakoutas, A practical method for determining shear crack induced deformation in FRP RC members, *Eng. Struct.* 126 (2016) 253–364.
- [5] A.A. Shukria, M.A. Hosen, R. Muhamad, M.Z. Jumaata, Behaviour of precracked RC beams strengthened using the side-NSM technique, *Constr. Build. Mater.* 123 (1) (2016) 617–626.
- [6] M. Frangou, K. Pilakoutas, S. Dritsos, Structural repair strengthening of RC columns, *Constr. Build. Mater.* 9 (5) (1995) 259–266.
- [7] T. Imjai, M. Setkit, R. Garcia, P. Sukontasukkul, S. Limkatanyu, Seismic strengthening of low strength concrete columns using high ductile metal strap confinement: a case study of kindergarten school in Northern Thailand, *Walailak J. Sci. Technol.* 18 (1) (2021).
- [8] C.K. Ma, A.Z. Awang, R. Garcia, W. Omar, K. Pilakoutas, Behaviour of over-reinforced high-strength concrete beams confined with post-tensioned steel straps—an experimental investigation, *Struct. Concr.* 17 (5) (2016) 768–777.
- [9] T. Imjai, C. Chaisakulkiet, R. Garcia, K. Pilakoutas, Strengthening of RC members using Post-Tensioned Metal Straps: state of the research, *Lowland Technol. Int. (LTI) J.* 20 (2) (2018) 187–196.
- [10] M. Setkit, T. Imjai, Strengthening performance of damaged concrete beams in service conditions using post-tensioned metal strapping technique, *J. King Mongkut's Univ. Technol. North Bangkok* 29 (4) (2019) 577–584.
- [11] R. Garcia, et al., Seismic retrofitting of RC buildings using CFRP and post-tensioned metal straps: shake table tests, *Bull. Earthq. Eng.* 15 (8) (2017) 3321–3347.
- [12] R. Parretti, A. Nanni, Strengthening of RC members using near-surface mounted FRP composites: design overview, *Adv. Struct. Eng.* 7 (6) (2004) 469–483.
- [13] L. De Lorenzis, J.G. Teng, Near-surface mounted FRP reinforcement: an emerging technique for strengthening structure, *Compos. Part B* 38 (2) (2007) 119–143.
- [14] W.T. Jung, Y.H. Park, J.S. Park, J.Y. Kang, Y.J. You, Experimental Investigation on Flexural Behaviour of RC Beams Strengthened by NSM CFRP Reinforcements, *ACI Special Publication*, ACI-SP-230, 2005.
- [15] F. Mahmoud, Castel, A.R. Francois, C. Tourneur, Strengthening of RC members with near-surface mounted CFRP rods, *Compos. Struct.* 91 (2) (2009) 138–147.
- [16] M.D.A. Housen, M.Z. Jumaat, A.B.M. Saiful Islan, Side near surface mounted (SNSM) technique for flexural enhancement of RC beams, *Mater. Des.* 83 (2015) 587–597.
- [17] A.M. Morsy, E.M. El-Tony, M. El-Naggar, Flexural repair/strengthening of pre-damaged R.C. beams using embedded CFRP rods, *Alexandria Eng. J.* 54 (4) (2015) 1175–1179.
- [18] ACI Committee 318, *Building Code Requirements for Structural Concrete: (ACI 318-19); and Commentary (ACI 318R-19)*, American Concrete Institute, Farmington Hills, MI, 2019.
- [19] British Standard Institution, BS 1881-116:1983 Testing Concrete - Part 116: Method for Determination of Compressive Strength of Concrete Cubes, BSI, London, UK, 1983.
- [20] British Standard Institution, BS 1881-117:1983 Testing Concrete - Part 117: Method for Determination of Tensile Splitting Strength, BSI, London, UK, 1983.
- [21] British Standard Institution, BS 1881-118:1983 Testing Concrete - Part 118: Method for Determination of Flexural Strength, BSI, London, UK, 1983.
- [22] R. Garcia, I. Hajirasouliha, M. Guadagnini, Y. Helal, Y. Jemaa, K. Pilakoutas, P. Mongabure, C. Chrysostomou, N. Kyriakides, A. Ilki, M. Budescu, Full-scale shaking table tests on a substandard RC building repaired and strengthened with Post-Tensioned Metal Straps, *J. Earthq. Eng.* 18 (2) (2014) 187–213.
- [23] D.E. Branson, Deflections of Reinforced Concrete Flexural Members, ACI Committee Report, ACI-435.2R-66 (re-approved 1989), Detroit, 1966 29 pp..
- [24] Federation International du Beton, *fib Model Code for Concrete Structures 2010*, Wilhelm Ernst & Sohn, Berlin, 2013.